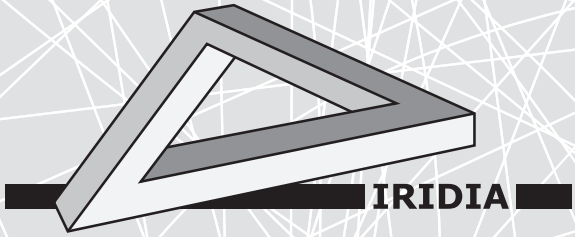

Université Libre de Bruxelles

Institut de Recherches Interdisciplinaires
et de Développements en Intelligence Artificielle

Frankenstein's PSO: A Composite Particle Swarm Optimization Algorithm

Marco A. Montes de Oca, Thomas Stützle,
Mauro Birattari and Marco Dorigo

IRIDIA – Technical Report Series

Technical Report No.
TR/IRIDIA/2007-006

March 2007

IRIDIA – Technical Report Series
ISSN 1781-3794

Published by:
IRIDIA, *Institut de Recherches Interdisciplinaires et de Développements en Intelligence Artificielle*
Université Libre de Bruxelles
Av F. D. Roosevelt 50, CP 194/6
1050 Bruxelles, Belgium

Technical report number TR/IRIDIA/2007-006

Revision history:
TR/IRIDIA/2007-006.001 March 2007
TR/IRIDIA/2007-006.002 January 2008

Frankenstein's PSO: A Composite Particle Swarm Optimization Algorithm

Marco A. Montes de Oca mmontes@ulb.ac.be
Thomas Stützle stuetzle@ulb.ac.be
Mauro Birattari mbiro@ulb.ac.be
Marco Dorigo mdorigo@ulb.ac.be
IRIDIA, Université Libre de Bruxelles, Brussels, Belgium

January 2008

Abstract

During the last decade, many modifications of the original particle swarm optimization (PSO) algorithm have been proposed. In many cases, it is claimed that the modified variant is superior to some reference variant in some way. The differences between two variants can often be seen as an algorithmic component being present in one variant but not in the other. From this perspective, the question arises as to whether it is possible to integrate different algorithmic components into a single PSO variant that performs better than the variants from which its components are taken.

In this paper, we take this perspective to design a new PSO algorithm whose components were selected after a careful evaluation of their impact on optimization speed and reliability. We call this composite algorithm *Frankenstein's PSO* in an analogy to the popular character of Mary Shelley's novel. The evaluation of Frankenstein's PSO performance suggests that the answer to the driving question is positive.

We present the process that guided us in selecting and adapting the algorithmic components included in Frankenstein's PSO. The performance of the composite algorithm is validated via a comparison with the variants from which the components were taken on a number of well-known benchmark problems.

1 Introduction

Since particle swarm optimization (PSO) was introduced [1, 2], many researchers have proposed modifications to the original algorithm (for reviews see [3] and [4]). In many cases, the modifications are algorithmic components that are included to provide an improved performance. The nature of these algorithmic components ranges from added constants in the particles' velocity update rule [5] to stand-alone algorithms that are used as components of hybrid PSO algorithms [6].

Over the years, almost all effort has been devoted to study the effects of different components on the behavior of a PSO algorithm (although not exactly from this perspective); however, little or no effort has been put into the study of

the possible interactions between algorithmic components. The explicit study of these interactions provides the possibility of improving our understanding of the PSO approach in general and helps in the task of designing more effective PSO algorithms.

This paper is organized in two parts. First, we carry out a comparison of some PSO variants on a set of common benchmark problems. The comparison is based on a detailed empirical performance analysis from which we identify algorithmic components that provide a positive effect on some performance aspect. Second, we design and evaluate a new composite algorithm, called *Frankenstein's PSO*, which integrates the algorithmic components that were identified during the first phase. The final evaluation consists in comparing Frankenstein's PSO with the variants from which its components were taken.

The experimental setup and the choice of the PSO variants allow the identification of performance differences that can be ascribed to specific algorithmic components. Our comparison focuses on the differences between mechanisms for updating a particle's velocity, although other factors such as the selection of the population topology, the number of particles and the strategies for updating at run-time various parameters that influence performance are also considered. The comparison of PSO variants is performed with their most commonly used parameter settings (i.e., those commonly found in the literature).

Algorithm composition is an approach to the study of the effects of algorithmic components and their interactions. The results presented in this paper show that high-performance PSO algorithms can be assembled in this way.

2 Particle Swarm Optimization Algorithms

To optimize a d-dimensional continuous objective function $f : \mathbb{R}^d \to \mathbb{R}$, a population of particles $\mathcal{P} = \{p_1, \ldots, p_n\}$ (called *swarm*) is randomly initialized in the solution space. The objective function determines the quality of the solution represented by a particle's position. (Without loss of generality, we restrict the following discussion to minimization problems.)

At any time step t, a particle p_i has an associated position vector $\boldsymbol{x}_i^t$ and a velocity vector $\boldsymbol{v}_i^t$. A vector $\boldsymbol{pb}_i^t$ (known as *personal best*) stores the best position the particle has ever visited. Particle p_i is said to have a topological neighborhood $\mathcal{N}_i \subseteq \mathcal{P}$ of particles. The best *personal best* vector in a particle's neighborhood (called *local best*) is a vector $\boldsymbol{lb}_i^t$ such that $f(\boldsymbol{lb}_i^t) \leq f(\boldsymbol{pb}_j^t)\, \forall p_j \in \mathcal{N}_i$.

PSO algorithms update the particles' velocities and positions iteratively until a stopping criterion is met. The basic velocity- and position-update rules are:

$$\boldsymbol{v}_i^{t+1} = \boldsymbol{v}_i^t + \varphi_1 \boldsymbol{U}_1^t (\boldsymbol{pb}_i^t - \boldsymbol{x}_i^t) + \varphi_2 \boldsymbol{U}_2^t (\boldsymbol{lb}_i^t - \boldsymbol{x}_i^t)\,, \tag{1}$$

and

$$\boldsymbol{x}_i^{t+1} = \boldsymbol{x}_i^t + \boldsymbol{v}_i^{t+1}\,, \tag{2}$$

where φ_1 and φ_2 are two parameters called the *cognitive* and *social* acceleration coefficients respectively, $\boldsymbol{U}_1^t$ and $\boldsymbol{U}_2^t$ are two $d \times d$ diagonal matrices with in-diagonal elements distributed in the interval $[0, 1)$ uniformly at random. (These matrices are generated at every iteration.) It was soon noticed that a particle's

velocity tended to grow beyond useful limits, so a maximum velocity parameter V_{max} was introduced to prevent velocities from growing to extremely large values [7, 8].

In the following paragraphs, we describe the variants that are part of our study. Inevitably, there is a personal factor involved in the selection; however, we believe the chosen variants are among the most influential and promising ones.

2.1 Constricted Particle Swarm Optimizer

Clerc and Kennedy [5] added a *constriction factor* to the particles' velocity-update rule to avoid the unlimited growth of the particles' velocity. Eq. 1 is modified to

$$\boldsymbol{v}_i^{t+1} = \chi \left(\boldsymbol{v}_i^t + \varphi_1 \boldsymbol{U}_1^t (\boldsymbol{pb}_i^t - \boldsymbol{x}_i^t) + \varphi_2 \boldsymbol{U}_2^t (\boldsymbol{lb}_i^t - \boldsymbol{x}_i^t) \right), \tag{3}$$

with $\chi = 2/\left|2 - \varphi - \sqrt{\varphi^2 - 4\varphi}\right|$ where χ is the constriction factor, $\varphi = \sum_i \varphi_i$ and $\varphi > 4$. Usually, φ_1 and φ_2 are set to 2.05, giving as a result χ equal to 0.729 [8, 9]. This variant will be referred to as *constricted* PSO in the rest of the article.

2.2 Time-Varying Inertia Weight Particle Swarm Optimizers

Shi and Eberhart [10, 11] noticed that the first term of the right hand side of Eq. 1 plays the role of a particle's "inertia" and they introduced the idea of an *inertia weight*. The velocity-update rule was modified to

$$\boldsymbol{v}_i^{t+1} = w^t \boldsymbol{v}_i^t + \varphi_1 \boldsymbol{U}_1^t (\boldsymbol{pb}_i^t - \boldsymbol{x}_i^t) + \varphi_2 \boldsymbol{U}_2^t (\boldsymbol{lb}_i^t - \boldsymbol{x}_i^t), \tag{4}$$

where w^t is the time-dependent inertia weight. Shi and Eberhart proposed to set the inertia weight according to a time-decreasing function so as to have an algorithm that initially explores the search space and only later focuses on the most promising regions. Experimental results showed that this approach is effective [7, 10, 11]. The function used to schedule the inertia weight is defined as

$$w^t = \frac{wt_{max} - t}{wt_{max}} (w_{max} - w_{min}) + w_{min}, \tag{5}$$

where wt_{max} marks the time at which $w^t = w_{min}$; w_{max} and w_{min} are the maximum and minimum values the inertia weight can take, respectively. Normally, wt_{max} coincides with the maximum time allocated for the optimization process. We identify this variant as *decreasing-IW* PSO. The constricted PSO can be considered a special case of this variant but with a constant inertia weight. We treat them as different variants because of their different behavior and for historical reasons.

Zheng et al. [12, 13] studied the effects of using a time-increasing inertia weight function obtaining, in some cases, better results than the decreasing-IW variant. Concerning the schedule of the inertia weight, Zheng et al. also used Eq. 4, except that the values of w_{max} and w_{min} were interchanged. This variant is referred to as *increasing-IW* PSO.

Eberhart and Shi [14] proposed a variant in which an inertia weight vector is randomly generated according to a uniform distribution in the range [0.5,1.0) with a different inertia weight for each dimension. This range was inspired by Clerc and Kennedy's constriction factor because the expected value of the inertia weight in this case is $0.75 \approx 0.729$. Accordingly, in this *stochastic-IW* PSO algorithm, acceleration coefficients are set to the product of $\chi \cdot \varphi_i$ with $i \in \{1, 2\}$.

2.3 Fully Informed Particle Swarm Optimizer

Mendes et al. [15] proposed the fully informed particle swarm (FIPS), in which a particle uses information from all its topological neighbors. Clerc and Kennedy's constriction factor is also adopted in FIPS; however, the value φ (i.e., the sum of the acceleration coefficients) is equally distributed among all the neighbors of a particle.

For a given particle p_i, φ is decomposed as $\varphi_k = \varphi/|\mathcal{N}_i|\,,\ \forall p_k \in \mathcal{N}_i$. As a result, the velocity-update equation becomes

$$\boldsymbol{v}_i^{t+1} = \chi \left[\boldsymbol{v}_i^t + \sum_{p_k \in \mathcal{N}_i} \varphi_k \boldsymbol{U}_k^t (\boldsymbol{pb}_k^t - \boldsymbol{x}_i^t) \right] . \tag{6}$$

2.4 Self-Organizing Hierarchical Particle Swarm Optimizer with Time-varying Acceleration Coefficients

Ratnaweera et al. [16] proposed the self-organizing hierarchical particle swarm optimizer with time-varying acceleration coefficients (HPSOTVAC), in which the inertia term in the velocity-update rule is eliminated. Additionally, if any component of a particle's velocity vector becomes zero (or very close to zero), it is reinitialized to a value proportional to V_{max}, the maximum velocity allowed. This gives the algorithm a local search behavior that is amplified by linearly adapting the value of the acceleration coefficients φ_1 and φ_2. The cognitive coefficient φ_1 is decreased from 2.5 to 0.5 and the social coefficient φ_2 is increased from 0.5 to 2.5. In HPSOTVAC, the maximum velocity is linearly decreased during a run so as to reach one tenth of its value at the end. A low reinitialization velocity near the end of the run allows particles to move slowly near the best region they have found. The resulting PSO variant is a kind of local search algorithm with occasional magnitude-decreasing unidimensional restarts.

2.5 Adaptive Hierarchical Particle Swarm Optimizer

Differently from the other variants, the adaptive hierarchical PSO (AHPSO) [17] modifies the neighborhood topology at run time. It uses a tree-like topology structure in which particles with better objective function evaluations are located in the upper nodes of the tree. At each iteration, a child particle updates its velocity considering its own previous best performance and the previous best performance of its parent. Before the velocity-update process takes place, the previous best fitness value of any particle is compared with that of its parent. If it is better, child and parent swap their positions in the hierarchy. Additionally, AHPSO adapts the branching degree of the tree while solving a problem

to balance the exploration-exploitation behavior of the algorithm: a hierarchy with a low branching degree has a more exploratory behavior than a hierarchy with a high branching degree. In AHPSO, the branching degree is decreased by k_{adapt} degrees (one at a time) until a certain minimum degree d_{min} is reached. This process takes place every f_{adapt} number of iterations. For more details, see [17].

3 Experimental Setup

The focus of the comparison is on the impact on performance of different mechanisms for updating a particle's velocity. However, other factors are also considered. The complete experimental design examines five factors:

1. **PSO algorithm**. This factor considers the differences between PSO variants. Specifically, we focused on (i) different strategies for updating inertia weights, (ii) the use of static and time-varying population topologies and (iii) different strategies for updating a particle's velocity.

2. **Problem**. We selected some of the most commonly used benchmark functions in experimental evolutionary computation. Since most of these functions have their global optimum located at the origin, we shifted it to avoid any possible search bias as suggested by Liang et al. [18]. In most cases, we used the shift values proposed in the set of benchmark functions used for the special session on real parameter optimization of the IEEE CEC 2005 [19]. Table 1 lists the benchmark functions used in our study. In all cases, we used their 30-dimensional versions. (Their definitions can be found in this paper's supplementary information web page [20][1].) All algorithms were run 100 times on each problem.

Table 1: Benchmark Problems

Function Name	Search Range	Modality
Ackley	$[-32.0, 32.0]^n$	Multimodal
Griewank	$[-600.0, 600.0]^n$	Multimodal
Rastrigin	$[-5.12, 5.12]^n$	Multimodal
Salomon	$[-100.0, 100.0]^n$	Multimodal
Schwefel (sine root)	$[-512.0, 512.0]^n$	Multimodal
Step	$[-5.12, 5.12]^n$	Multimodal
Rosenbrock	$[-30.0, 30.0]^n$	Unimodal
Sphere	$[-100.0, 100.0]^n$	Unimodal

3. **Population topology**. We use three of the most commonly used population topologies: The fully connected topology, in which every particle is a neighbor of any other particle in the swarm; the square topology, in which each particle is a neighbor of 4 other particles; and the ring topology, in which each particle is a neighbor of another 2 particles. In our setup, all particles are also neighbors to themselves. These three topologies are tested with all variants except in the case of AHPSO which uses a

[1] At this same address the reader can find all the supporting supplementary information (definitions, tables and graphs) that, for the sake of conciseness, we do not present here.

time-varying topology. The selected topologies provide different degrees of connectivity between particles. The goal is to favor exploration in different degrees: The less connected is a topology, the more it delays the propagation of the best-so-far solution. Thus, low connected topologies result in more exploratory behavior than highly connected ones [21]. Although recent research suggests that random topologies can be competitive to predefined ones [22], they are not included in our setup in order not to have an unmanageable number of free variables.

4. **Population size**. We considered three population sizes: 20, 40 and 60 particles. With low connected topologies and large populations, the propagation of information is slower and thus it is expected that a more "parallel" search takes place. Square topologies can have different configurations for the same number of particles. The configurations that we considered for 20, 40 and 60 particles were 5×4, 5×8 and 6×10 respectively. The population is initialized uniformly at random over the ranges specified in Table 1. Since the problems' optima were shifted, the initialization range is asymmetric with respect to them.

5. **Maximum number of function evaluations**. This factor determined the stopping criterion. The limit was set to 10^6 function evaluations. However, data were collected during a run to determine relative performances for shorter runs. The goal was to find variants that are well suited for different application scenarios. The first two cases (10^3 and 10^4 function evaluations) model scenarios in which there are scarce resources and the best possible solution is sought given a restrictive time limit. The other two cases (10^5 and 10^6 function evaluations) model scenarios in which the main concern is to find high quality solutions without paying too much attention to the time it takes to find them.

In our experimental setup, each algorithm was run with the same parameter settings across all benchmark problems. When possible, we use the most commonly used parameter settings found in the literature. These parameter settings are listed in Table 2.

In our experimental analysis, we examined the algorithms' performance at different levels of aggregation. At a detailed level, we analyze the algorithms' qualified run-length distributions (RLDs, for short). At a more aggregate level, we use the median solution quality reached by the algorithms at different stopping criteria. The most important elements of the RLD methodology are explained below (for a detailed exposition, see [23]).

The number of function evaluations needed by a stochastic optimization algorithm to find a solution of a certain quality on a given problem can be modeled as a random variable. Its associated cumulative probability distribution is the algorithm's RLD.

Formally, an algorithm's RLD is denoted by $RL_q(l)$ and is defined as

$$RL_q(l) = P(L_q \leq l)\,, \tag{7}$$

where L_q is the random variable representing the number of function evaluations needed to find a solution of quality q, and $P(L_q \leq l)$ is the probability that L_q takes a value less than or equal to a certain number of evaluations l.

Table 2: Parameter settings

Algorithm	Settings
Constricted	Acceleration coefficients $\varphi_1 = \varphi_2 = 2.05$. Constriction factor $\chi = 0.729$. Maximum velocity $V_{max} = \pm X_{max}$, where X_{max} is the maximum of the search range.
Decreasing-IW	Acceleration coefficients $\varphi_1 = \varphi_2 = 2.0$. Linearly-decreasing inertia weight from 0.9 to 0.4. The final value is reached at the end of the run. Maximum velocity $V_{max} = \pm X_{max}$.
Increasing-IW	Acceleration coefficients $\varphi_1 = \varphi_2 = 2.0$. Linearly-increasing inertia weight from 0.4 to 0.9. The final value is reached at the end of the run. Maximum velocity $V_{max} = \pm X_{max}$.
Stochastic-IW	Acceleration coefficients $\varphi_1 = \varphi_2 = 1.494$. Uniformly distributed random inertia weight in the range $[0.5, 1.0]$. Maximum velocity $V_{max} = \pm X_{max}$.
FIPS	Acceleration parameter $\varphi = 4.1$. Constriction factor $\chi = 0.729$. Maximum velocity $V_{max} = \pm X_{max}$.
HPSOTVAC	Acceleration coefficient φ_1 linearly decreased from 2.5 to 0.5 and coefficient φ_2 linearly increased from 0.5 to 2.5. Linearly decreased reinitialization velocity from V_{max} to $0.1 \cdot V_{max}$. Maximum velocity $V_{max} = \pm X_{max}$.
AHPSO	Acceleration coefficients $\varphi_1 = \varphi_2 = 2.05$. Constriction factor $\chi = 0.729$. Initial branching factor is set to 20, d_{min}, f_{adapt}, and k_{adapt} were set to 2, $1000 \cdot m$, and 3 respectively, where m is the number of particles.

Theoretical RLDs are estimated empirically using multiple independent runs of an algorithm.

An empirical RLD provides a graphical view of the development of the probability of finding a solution of a certain quality as a function of time. When this probability does not increase or it does but very slowly, the algorithm is said to stagnate. In this paper we use the word stagnation to refer to the phenomenon of slow or no improvement of the solution quality over time or, as in this case, to the slow or no increment of the probability of finding a solution of a specific quality. Note that no reference to the state of the optimization algorithm is implied.

In stagnation cases, the probability of finding a solution of a certain quality can be increased by restarting the algorithm at fixed intervals of time instead of letting it run for longer. A restart is the process of rerunning the algorithm using the same parameter settings without passing over any information from the previous run and using a different sequence of random numbers.

The RLD of an algorithm that is restarted periodically will approximate, in the long run, an exponential distribution. However, when an algorithm's original RLD grows faster than an exponential distribution, the use of independent restarts is detrimental. It is possible to estimate, from an empirically estimated RLD, the number of function evaluations needed to find the required solution with a probability greater than or equal to z if an optimal restart policy is supposed to be used. This estimation is sometimes called *computational effort* [24] and it is defined as

$$\mathit{effort} = \min_{l} \left\{ l \cdot \frac{ln(1-z)}{ln(1-RL_q(l))} \right\}. \tag{8}$$

We use this measure to complement our analysis by considering the possibility of restarting the compared algorithms with optimal restart policies.

Fig. 1 shows an example RLD of an algorithm with and without restarts together with the exponential distribution that the algorithm with restarts is ideally following. Both the cut-off time and the estimated effort for a probability of $z = 0.99$ are indicated with arrows.

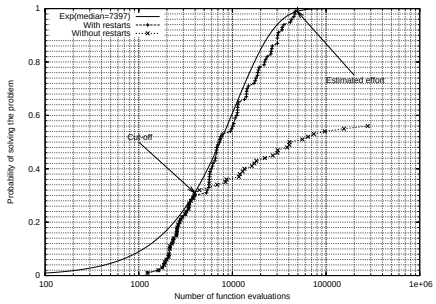

Figure 1: Example of empirical RLDs of an algorithm with and without restarts. See the text for more details.

Another measure that will be used in the description of the results is the *first hitting time* H_q for a specific solution quality q. H_q is an estimation of the minimum number of evaluations that an algorithm needs for finding a solution

of a quality level q. It is defined as

$$H_q = \min\{l \geq 0; RL_q(l) > 0\}\,. \tag{9}$$

4 Performance Comparison of Particle Swarm Optimization Algorithms

The comparison is carried out in three phases. In the first one, a problem-dependent run-time behavior comparison based on RLDs is performed (a preliminary series of results is published in [25]). In the second phase, data from all the problems of our benchmark suite are aggregated and analyzed. In the third phase, we study the effects of using different inertia weight schedules on the performance of the concerned variants. Results that are valid for all the tested problems are explicitly summarized.

4.1 Results: Run-Length Distributions

The graphs presented in this section show a curve for each of the compared algorithms corresponding to a particular combination of a population topology and a population size. Since AHPSO does not use a fixed topology, its RLDs are the same across topologies and its results can therefore be used as a reference across plots for a same problem. The RLDs we present here were obtained using swarms of 20 and 60 particles.

Because of space constraints, we present only one representative example of the results we obtained. Fig. 2 shows some of the algorithms' RLDs when solving Griewank's function. These plots are given with respect to a bound of 0.001% above the optimum value, corresponding to an absolute error of 0.0018. The smallest first hitting times for the same algorithm across different population size and topology settings are obtained with a population size of 20 and the fully connected topology. Conversely, the largest ones are obtained with a population size of 60 and the ring topology. With 20 particles, the right tails of the RLDs show a slowly-increasing or a non-increasing slope. This means that with 20 particles all PSO variants have a strong stagnation tendency in this problem. In fact, no variant is capable of finding a solution of the required quality with a probability of 1.0 with this population size. With 60 particles and a ring topology, only FIPS finds the required solution quality with a probability of 1.0, while the constricted PSO and HPSOTVAC reach a solution of the required quality with a probability of 0.99.

Result 1: *Depending on the problem and required solution quality, PSO algorithms exhibit a stagnation tendency with different degrees of severity. This tendency is smaller when using large population sizes and/or low connected topologies than it is when using small population sizes and/or highly connected topologies. However, even though the probability of solving the problem increases, first hitting times are normally delayed.*

An interesting fact is the strong influence of the topology on the algortihms' performance. For example, FIPS with a fully connected topology does not find a single solution of the required quality; however, with a ring topology, it is among the fastest algorithms (in terms of the first hitting times). AHPSO seems to profit from a highly connected topology at the beginning of a run. It is also

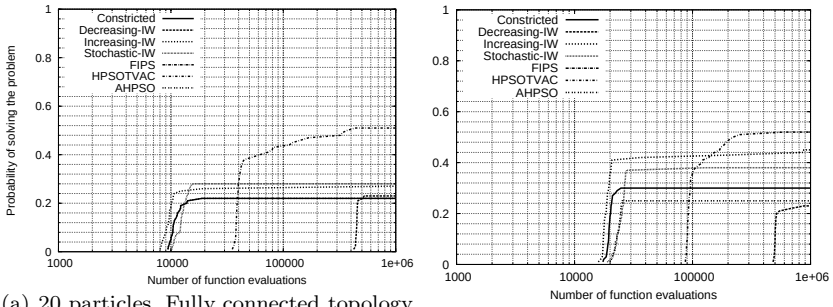

(a) 20 particles, Fully connected topology (b) 60 particles, Fully connected topology

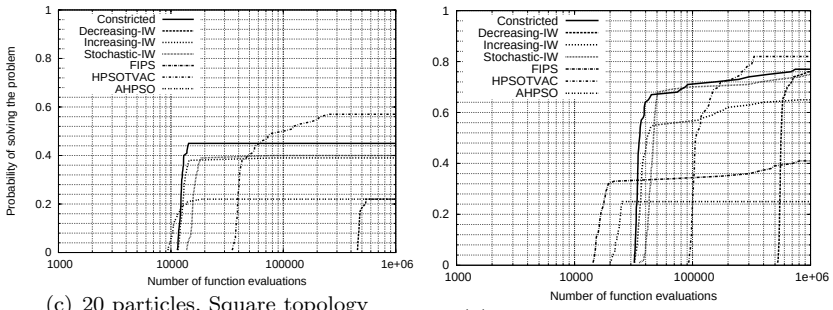

(c) 20 particles, Square topology (d) 60 particles, Square topology

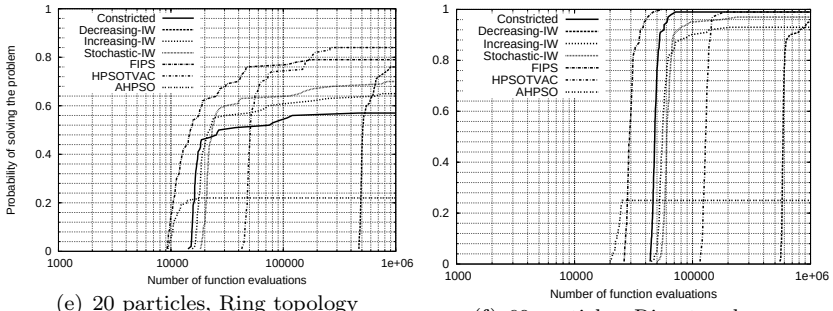

(e) 20 particles, Ring topology (f) 60 particles, Ring topology

Figure 2: RLDs on Griewank's function. The solution quality bound is set to 0.001% above the global optimum (equivalent to an absolute error of 0.0018). Plots (a), (c), and (e) in the left column show the RLDs obtained with 20 particles. Plots (b), (d), and (f) in the right column show the RLDs obtained with 60 particles. The effect of using different population topologies can be seen by comparing plots in different rows. The effect of using a different number of particles can be seen by comparing columns.

among the fastest variants when the rest of the algorithms use a square or ring topology. However, it is unable to solve the problem with a high probability.

FIPS's poor performance with a fully connected topology could be explained by looking at the evolution of the average distance of the particles' previous best positions to their centroid (a measure of convergence in space). Fig. 3 shows the development of this measure over time on Griewank's problem. FIPS with a fully connected topology drives the swarm of particles to a single point in space much faster than with other topologies. Recently, it has been suggested that FIPS with a fully connected topology exhibits a random behavior [4]. However, our empirical results show that the distance between particles decreases over time and that the decrement is faster when the fully connected topology is used. Consequently, we believe that FIPS's poor behavior is actually due to the collapse of the swarm in the search space and not to a random behavior. It is worth to mentioning that this behavior is observed on all the tested functions.

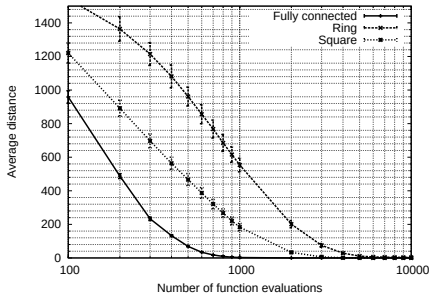

Figure 3: Evolution of the average distance of the particles' previous best positions to their centroid for FIPS solving Griewank's function with different topologies and 20 particles. The graph shows the mean and the standard deviation over 100 runs.

Result 2: *PSO algorithms are sensitive to a change in the population topology in different degrees. Among those tested, FIPS is the most sensitive variant to a change of this nature. On the contrary, HPSOTVAC and the decreasing inertia weight PSO algorithm are quite stable to topology changes.*

As a best-case analysis, we now consider the possibility of restarting the algorithms with an optimal restart policy. In order to estimate the number of function evaluations needed to find the required solution quality with a certain probability, we use Eq. 8. In Table 3 we show the best configuration of each algorithm to solve Griewank's problem (at 0.001% above the global optimum) with a probability of 0.99. The best performing configurations of FIPS and the constricted PSO, both with 60 particles and the ring topology, do not benefit from restarts under these conditions, and they are the two best variants for the considered goal. In this case, the joint effect of choosing the right algorithm, with an appropriate population size and with the right topology, cannot be outperformed by configurations that benefit from restarts (i.e., those that stagnate).

The effect of using restarts is algorithm- and problem-dependent. As an example, consider the data shown in Table 4. This table shows the best configuration of each algorithm to solve Rastrigin's problem (at 20.0% above the global optimum) with a probability of 0.99. Differently from what was observed

Table 3: Best performing configurations of each algorithm using independent restarts on Griewank's function[1, 2]

Algorithm	Pop. Size	Topology	Cut-off	Effort	Restarts
FIPS	60	Ring	46440	**46440**	0
Constricted	60	Ring	71880	71880	0
Sto-IW	40	Ring	52160	131075	2
Inc-IW	20	Ring	24040	138644	5
HPSOTVAC	40	Ring	132080	155482	1
AHPSO	40	Dynamic	17360	207295	11
Dec-IW	60	Ring	663000	1326000	1

[1] Probabilities taken from the RLDs.
[2] Cut-off and effort measured in function evaluations. The effort is computed using Eq. 8.

in the previous case, the best performing variants use a configuration with a strong stagnation tendency that benefits from restarts.

Table 4: Best performing configurations of each algorithm using independent restarts on the Rastrigin function[1, 2]

Algorithm	Pop. Size	Topology	Cut-off	Effort	Restarts
Inc-IW	40	Fully connected	12760	**41176**	3
Sto-IW	60	Square	50220	59119	1
Constricted	40	Square	17880	61126	3
AHPSO	60	Adaptive	18660	63792	3
HPSOTVAC	20	Ring	70220	70220	0
FIPS	40	Square	38640	93797	2
Dec-IW	20	Fully connected	460200	460200	0

[1] Probabilities taken from the RLDs.
[2] Cut-off and effort measured in function evaluations. The effort is computed using Eq. 8.

Result 3: *Independent restarts can improve the performance of various PSO algorithms. In some cases, configurations that favor an exploitative behavior can outperform those that favor an exploratory one if optimal restart policies are used. However, the optimal restart policy is algorithm- and problem-dependent and therefore cannot be defined a priori.*

4.2 Results: Aggregated Data

The analysis that follows is based on the median solution quality achieved by an algorithm after some specific number of function evaluations. This analysis considers only the 40 particles case which represents the intermediate case in terms of population size in our experimental setup. For each problem, we ranked 19 configurations (6 PSO algorithms $\times$ 3 topologies + AHPSO) and selected only those that were ranked in the first three places (what we call the top-three group). For this analysis, we assume that the algorithms are neither restarted nor fine-tuned for any specific problem.

Table 5 shows the distribution of appearances of the compared PSO algorithms in the top-three group. The table shows configurations ranked among the three best algorithms for different numbers of function evaluations (FES). The topology used by a particular configuration is shown in parenthesis. If two or more configurations found solutions with the same quality level (differences

smaller than 10^{-15} are not considered) and they were among the three best solution qualities, these configurations were considered to be part of the top-three group. In fact, we observed that, as the number of function evaluations increases, more and more algorithms appear in the top-three group. This indicates that the difference in the solution quality achieved by different algorithms decreases and that many algorithms achieve the same quality level.

Table 5: Distribution of appearances of different PSO algorithms in the top-three group[1]

FES	Ackley	Griewank	Rastrigin	Salomon	Schwefel	Step	Rosenbrock	Sphere
10^3	FIPS (F,S) Inc-IW (F)	FIPS (F,S) Inc-IW (F)	FIPS (F,S) Inc-IW (F)	FIPS (F,S) HPSOTVAC	Inc-IW (F,S,R)	FIPS (F,S) Inc-IW (F)	AHPSO Constricted (F) Sto-IW (F)	FIPS (F,S) Inc-IW (F)
10^4	FIPS (S,R) Inc-IW (F)	Constricted (F) FIPS (S) Inc-IW (F)	AHPSO Constricted (F) Inc-IW (F)	Constricted (F) Inc-IW (F) Sto-IW (F)	AHPSO Inc-IW (F) Sto-IW (F)	AHPSO Constricted (F) Inc-IW (F) Sto-IW (F)	AHPSO Constricted (F) Sto-IW (F)	AHPSO Constricted (F) Inc-IW (F)
10^5	Constricted (S) FIPS (R) Inc-IW (F)	Constricted (S,R) FIPS (R) Inc-IW (S,R) Sto-IW (S,R)	FIPS (S) Inc-IW (S) Sto-IW (S)	Constricted (S,R) FIPS (R) Inc-IW (F,S) Sto-IW (F,S,R)	HPSOTVAC (F,S,R)	Constricted (S) Inc-IW (F) Sto-IW (F)	AHPSO Constricted (F) Sto-IW (F)	AHPSO Constricted (F,S,R) FIPS (R) Inc-IW (F,S,R) Sto-IW (F,S,R)
10^6	Constricted (S,R) Dec-IW (F,S,R) FIPS (R) Inc-IW (S,R) Sto-IW (S,R)	Constricted (S,R) Dec-IW (S,R) FIPS (R) HPSOTVAC (F,S,R) Inc-IW (S,R) Sto-IW (S,R)	HPSOTVAC (F,S,R)	Constricted (S,R) Dec-IW (F,S,R) FIPS (R) HPSOTVAC (F,S,R) Inc-IW (S,R) Sto-IW (S,R)	Dec-IW (S) FIPS (R) HPSOTVAC (R)	Constricted (S,R) Dec-IW (F,S,R) FIPS (R) HPSOTVAC (F,S,R) Inc-IW (F,S,R) Sto-IW (F,S,R)	AHPSO Constricted (F) Sto-IW (F)	AHPSO Constricted (F,S,R) Dec-IW (F,S,R) FIPS (R) HPSOTVAC (S) Inc-IW (F,S,R) Sto-IW (F,S,R)

[1] F, S and R stand for fully connected, square and ring, respectively. FES stands for function evaluations.

Table 6 shows the algorithms that most often appear in the top-three group in Table 5 for different termination criteria. The column labeled "Σ" shows the total number of times each algorithm appeared in the top-three group. The rightmost column shows the distribution of appearances in the top-three group between multi- and unimodal functions.

Table 6: Best PSO variants for different termination criteria

Budget (in FES)	Algorithm(Topology)	Σ	multi/unimodal
10^3	Inc-IW(F), FIPS(F,S)	6	5/1
10^4	Inc-IW(F)	7	6/1
10^5	Constricted(S)	5	4/1
10^6	Dec-IW(S), FIPS(R)	6	5/1

Note that the connectivity of the topology used by the best ranked variants decreases as the maximum number of function evaluations increases. It is also interesting to note that FIPS is the best ranked algorithm in the shortest as well as in the longest runs. Our results extend those of Mendes [21] who studied the behavior of FIPS using only a fixed number of function evaluations as stopping criterion.

Result 4: *When a limited number of function evaluations are allowed, configurations that favor an exploitative behavior (i.e., those with highly connected topologies and/or low inertia weights) obtain the best results. When solution quality is the most important aspect, algorithms with exploratory properties are the best performing.*

4.3 Results: Different Inertia Weight Schedules

In the current literature, the change of the inertia weight value in the time-decreasing/increasing inertia weight variants is scheduled over the whole optimization process. In this section, we present a study on the effects of using different schedules. To do so, we modified the inertia weight schedule, which is based on Eq. 5, so that whenever the inertia weight reaches its limit value, it remains there. We experimented with five inertia weight schedules of $wt_{max} \in \{10^2, 10^3, 10^4, 10^5, 10^6\}$ function evaluations each. The remaining parameters were set as shown in Table 2.

As an example of the effects of different inertia weight schedules, consider Fig. 4, which shows the development of the solution quality over time (using both the time-decreasing and time-increasing inertia weight variants) for different inertia weight schedules on the Rastrigin function.

In the case of the time-decreasing inertia weight variant, slow schedules ($wt_{max} = 10^5$ or 10^6 function evaluations) perform poorly during the first phase of the optimization process; however, they are the ones that are capable of finding the best quality solutions. On the other hand, fast schedules ($wt_{max} = 10^2$ or 10^3 function evaluations) produce rapid improvement but at the cost of stagnation later in the optimization process.

With the time-increasing inertia weight variant, slow schedules provide the best performance. Fast schedules make the time-increasing inertia weight variant strongly stagnant. For both variants, the severity of the stagnation tendency induced by different schedules is alleviated by both an increase in the number of particles and the use of a low connected topology.

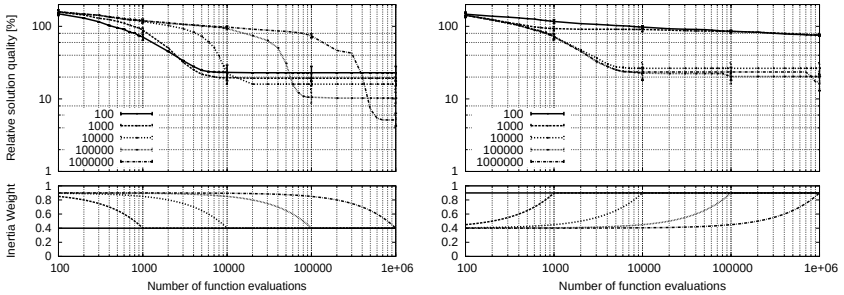

(a) Decreasing inertia weight (b) Increasing inertia weight

Figure 4: Solution quality and inertia weight development over time for different inertia weight schedules on the Rastrigin function. The solution quality development plots are based on the medians of the algorithms' RLDs. The first and third quartiles are shown at selected points. These results correspond to configurations of 20 particles in a fully connected topology.

Result 5: *By varying the inertia weight schedule, it is possible to control the convergence speed of the time-varying inertia weight variants. In the case of the time-decreasing inertia weight variant, faster schedules induce a faster convergence speed, albeit at the cost of increasing the algorithm's stagnation tendencies. In the time-increasing inertia weight variant, slow schedules provide the best performance both in terms of speed and quality.*

4.4 Summary

The goal of the comparison presented above was not to declare a winner PSO algorithm, but rather to identify algorithmic components that provide good performance under different operating conditions (specially run-lengths). The five main results give insight into what factors should be taken into account when trying to solve effectively a problem using a PSO algorithm.

Among other results, we have seen that stagnation tendencies of PSO algorithms can be alleviated by using a large population and/or low connected topologies. Another approach to reduce stagnation in some cases is to use restarts. However, optimal restart schedules are algorithm- and problem-dependent and determining them requires previous experimentation. We have also seen how different inertia weight schedules affect the performance of the time-varying inertia weight variants.

Some algorithmic components are of special importance due to the dramatic impact they have on the algorithms' performance. On some variants, some of these components have been relatively well studied (e.g., population topologies in the constricted PSO and FIPS); however, the interactions between different components on the algorithms' performance have not received sufficient attention.

5 Frankenstein's Particle Swarm Optimization Algorithm

Insights on experimental results ideally guide toward the definition of new, better performing algorithms. In this section, a composite algorithm called *Frankenstein's PSO* is assembled from algorithmic components that are taken from the PSO algorithms that we have examined or that are derived from the analysis of the comparison results. Since the goal is to design a PSO algorithm that works well regardless of the time allocated for the optimization process, the algorithmic components included in Frankenstein's PSO algorithm contribute to either find good quality solutions in short runs or find solutions of very good quality in long ones.

5.1 The Algorithm

Frankenstein's PSO is composed of three main algorithmic components, namely (i) a time-varying population topology that reduces its connectivity over time, (ii) FIPS's mechanism for updating a particle's velocity which successfully exploits topologies of varying degree of connectivity, and (iii) a decreasing inertia weight. Two of these components balance the exploration-exploitation behaviors during a run. The time-varying population topology enhances exploration over time and the decreasing inertia weight favors exploitation over time.

The time-varying topology starts as a fully connected one and, as the optimization process evolves, decreases its connectivity until it ends up being a ring topology. Interestingly, it is the opposite approach than the one taken by Suganthan [26]. Note, however, that our approach is entirely based on the results of the empirical analysis presented in the previous section. Specifically, our choice is based on the fact that a highly connected topology during the first iterations gives an algorithm the opportunity to find good quality solutions early in a run (see Table 6 and Results 1 and 4 in Section 4). The topology connectivity is then decreased, so that the risk of getting trapped somewhere in the search space is reduced and, hence, exploration is enhanced. Including this component into the algorithm permits the achievement of good performance across a wider range of run lengths as it will be shown later. A time-varying population topology is also found in AHPSO. Information flow in AHPSO is very fast during the first iterations because the topology connectivity is high. As the optimization process evolves, its connectivity decreases. In Frankenstein's PSO we do not use a hierarchical topology as it is not clear from our results whether it contributes to a good performance or not.

The topology is changed as follows. Suppose we have a particle swarm composed of n particles. We schedule the change of the topology so that in k iterations (with $k \geq n$), we transform a fully connected topology with $n(n-1)/2$ edges into a ring topology with n edges. The total number of edges that have to be eliminated are $n(n-3)/2$. Every $\lceil k/(n-3) \rceil$ iterations we remove m edges, where m of edges to remove follows an arithmetic regression pattern of the form $n-2, n-3, \ldots, 2$. We sweep m nodes removing one edge per node. The edge to be removed is chosen uniformly at random from the edges that do not belong to the exterior ring, which is predefined in advance (just as it is done when using the normal ring topology). The transformation from the initially

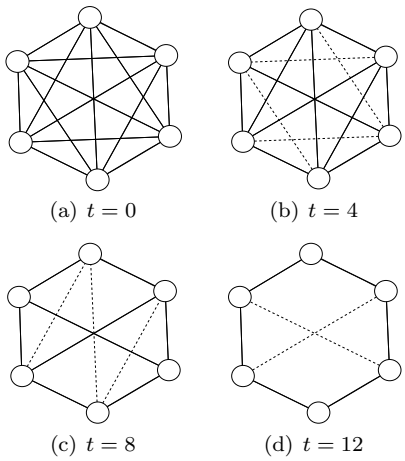

(a) $t = 0$ (b) $t = 4$

(c) $t = 8$ (d) $t = 12$

Figure 5: Topology change process. Suppose $n = 6$ and $k = 12$. Then, every $\lceil 12/(6-3) \rceil = 4$ iterations we remove some edges from the graph. In $6 - 3 = 3$ steps, the elimination process will be finished. (a). At $t = 0$ a fully connected topology is used. (b). At $t = 4$ the $6 - 2 = 4$ edges to be removed are shown in dashed lines. (c), at $t = 8$ the $6 - 3 = 3$ edges to be removed are shown in dashed lines. (d). At $t = 12$ the remaining $6 - 4 = 2$ edges to be removed are shown in dashed lines. From $t = 12$ on, the algorithm uses a ring topology.

fully connected to the final ring topology is performed in $n-3$ elimination steps. Fig. 5 shows a graphical example of how the process just described is carried out.

Changes in the population topology must be exploited by the underlying particles' velocity-update mechanism. In Frankenstein's PSO we included the mechanism used by FIPS. The reason for this is that we need a component that offers good performance across different topology connectivities. According to Table 6, the only velocity-update mechanism that is ranked among the best variants when using different topologies is the one used by FIPS. For short runs, FIPS's best performance is obtained with the fully connected topology (the way Frankenstein's PSO topology starts); for long runs, FIPS reaches very high performance with a low connected topology (the way Frankenstein's PSO topology ends).

The constriction factor originally used in FIPS is substituted by a decreasing inertia weight. A decreasing inertia weight was chosen because it is a parameter that can be used to control the algorithm's exploration/exploitation capabilities. In Section 4.3, we saw that a proper selection of the inertia weight schedule can dramatically change the performance of a PSO algorithm. A decreasing inertia weight would counterbalance the exploratory behavior that the chosen topology change scheme could induce.

The pseudocode of Frankenstein's PSO is shown in Algorithm 1. The main loop cycles through the three algorithmic components: topology update, inertia weight update, and the particles' velocity and position updates. The topology update mechanism is only executed while the algorithm's current number of iterations is lower than or equal to a parameter k, which specifies the topology update schedule. Since it is guaranteed that the ring topology is reached after

iteration k, there is no need to call this procedure thereafter. In Algorithm 1, a variable *esteps* is used to ensure that the number of eliminated edges in the topology follows an arithmetic regression pattern. Note that the elimination of neighborhood relations is symmetrical, that is, if particle r is removed from the neighborhood of particle i, particle i is also removed from the neighborhood of particle r. The inertia weight is then updated, and finally, the velocity-update mechanism is applied in the same way as in FIPS.

5.2 Parameterization Effects

We studied the impact of using different schedules for the topology and inertia weight updates on the algorithm's performance. The remaining parameters were the same as those used in the original context of the different algorithmic components, that is, the maximum velocity $V_{max} = \pm X_{max}$, the linearly-decreasing inertia weight is varied from 0.9 to 0.4, and the sum of the acceleration coefficients, φ, is set to 4.0.

The experimental conditions under which we evaluated the performance of the algorithm were the same that we used in the comparison of the different PSO algorithms. Three swarm sizes ($n = 20,\ 40,\ 60$), four schedules of the topology update (measured in iterations; $k = n,\ 2n,\ 3n,\ 4n$) and four schedules of the inertia weight (measured in function evaluations; $wt_{max} = n^2,\ 2n^2,\ 3n^2,\ 4n^2$) were tried. Note that the values of k and wt_{max} are independent from one another.

As an illustrative example of the results, consider Fig. 6. It shows the RLDs obtained by Frankenstein's PSO algorithm on Griewank's function. These distributions correspond, as before, to a solution quality 0.001% above the optimum value. Only the results obtained with 4 out of the 12 possible combinations of topology schedules and population sizes are shown[2].

A combination of a slow topology update schedule ($3n$ or $4n$) and a fast inertia weight schedule (n^2 or $2n^2$) promotes the stagnation of the algorithm. This can be explained if we recall that FIPS has a strong stagnation tendency when using a highly connected topology: A slow topology update schedule maintains a high topology connectivity for more iterations and a fast inertia weight schedule quickly reduces the exploration capabilities of the particle swarm. These two effects also increase the algorithm's stagnation tendency. To counteract a fast stagnation tendency, the two possibilities are to slow down the inertia weight schedule or to speed up the change of the topology.

Increasing the number of particles increases the amount of information available to the algorithm during the first iterations. The exploitation of this information depends on the topology update and inertia weight schedules. The configurations that appear to better exploit it are those in which these two schedules are slow.

Fig. 7 shows the average (over the 8 benchmark problems of the experimental setup) standard solution quality (i.e., for each group, the mean is equal to zero and the standard deviation is one) as a function of the topology update and the inertia weight schedules for different termination criteria. Since we work with minimization problems, a lower average standard solution quality means that the specific configuration found better solutions.

[2]We remind the reader that the full experimental data are available on our supplementary

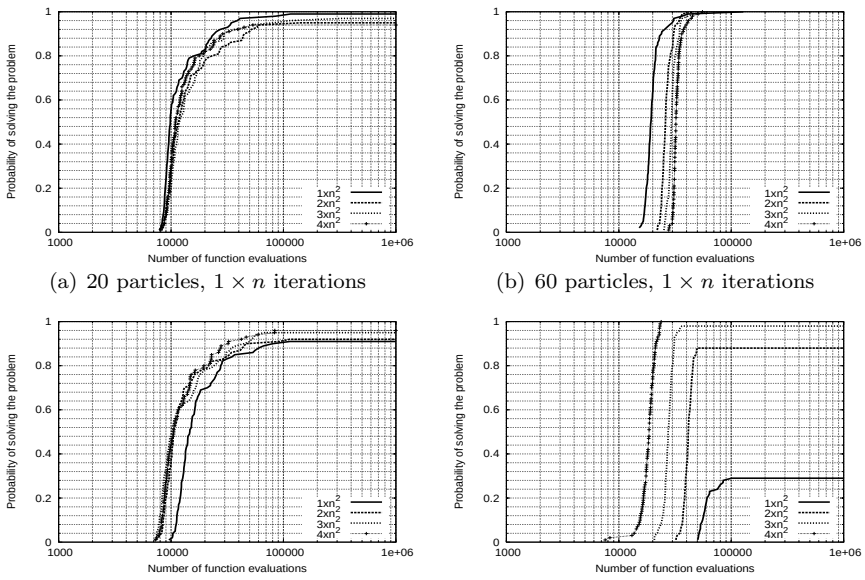

(a) 20 particles, $1 \times n$ iterations (b) 60 particles, $1 \times n$ iterations

(c) 20 particles, $4 \times n$ iterations (d) 60 particles, $4 \times n$ iterations

Figure 6: RLDs obtained by Frankenstein's PSO algorithm on Griewank's function. The solution quality demanded is 0.001% above the global optimum. Columns show the RLDs obtained with different number of particles. Rows show the RLDs obtained with different topology update schedules. Each graph shows four RLDs that correspond to different inertia weight schedules.

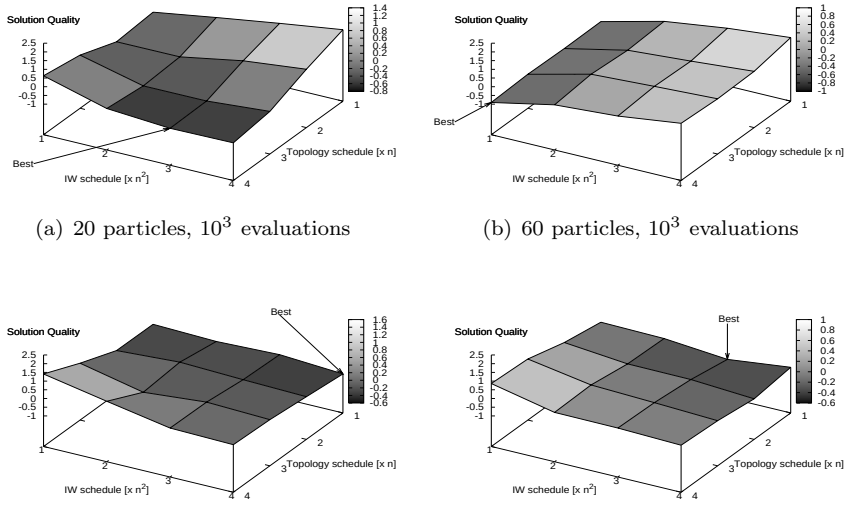

(a) 20 particles, 10^3 evaluations

(b) 60 particles, 10^3 evaluations

(c) 20 particles, 10^6 evaluations

(d) 60 particles, 10^6 evaluations

Figure 7: Average standard solution quality as a function of the topology update and the inertia weight schedules for different termination criteria. Columns show the results obtained with different number of particles. Rows show the results obtained for different termination criteria. In each case, the best configuration is pointed by an arrow.

Algorithm 1 Frankenstein's PSO algorithm

/* Initialization */
for $i = 1$ to n **do**
  Create particle p_i and add it to the set of particles $\mathcal{P}$
  Initialize its vectors $\boldsymbol{x}_i$ and $\boldsymbol{v}_i$ to random values within the search range and maximum allowed velocities
  Set $\boldsymbol{pb}_i = \boldsymbol{x}_i$
  Set $\mathcal{N}_i = \mathcal{P}$
end for

/* Main Loop */
Set $t = 0$
Set $esteps = 0$
repeat
  /* Evaluation Loop */
  for $i = 1$ to n **do**
    if $f(\boldsymbol{x}_i)$ is better than $f(\boldsymbol{pb}_i)$ **then**
      Set $\boldsymbol{pb}_i = \boldsymbol{x}_i$
    end if
  end for
  /* Topology Update */
  if $t > 0 \wedge t <= k \wedge t \bmod \lceil k/(n-3) \rceil = 0$ **then**
    /* $t > 0$ ensures that a fully connected topology is used first */
    /* $t <= k$ ensures that the topology update process is not called after iteration k */
    /* $t \bmod \lceil k/(n-3) \rceil = 0$ ensures the correct scheduling of the topology update process */
    for $i = 1$ to $n - (2 + esteps)$ **do**
      /* $n - (2 + esteps)$ ensures the arithmetic regression pattern */
      if $|\mathcal{N}_i| > 2$ **then**
        /* $|\mathcal{N}_i| > 2$ ensures proper node selection */
        Select at random particle p_r from $\mathcal{N}_i$ such that p_r is not adjacent to p_i
        Eliminate particle p_r from $\mathcal{N}_i$
        Eliminate particle p_i from $\mathcal{N}_r$
      end if
    end for
    Set $esteps = esteps + 1$
  end if
  /* Inertia Weight Update */
  if $t \leq iwt_{max}$ **then**
    Set $w(t) = \frac{wt_{max} - t}{wt_{max}}(w_{max} - w_{min}) + w_{min}$
  else
    Set $w(t) = w_{min}$
  end if
  /* Velocity and Position Update */
  for $i = 1$ to n **do**
    Generate $\boldsymbol{U}_m^t \ \forall p_m \in \mathcal{N}_i$
    Set $\varphi_m = \varphi / |\mathcal{N}_i| \ \forall p_m \in \mathcal{N}_i$
    Set $\boldsymbol{v}_i^{t+1} = w\, {}^t\boldsymbol{v}_i^t + \sum_{p_m \in \mathcal{N}_i} \varphi_k \boldsymbol{U}_k^t (\boldsymbol{pb}_k^t - \boldsymbol{x}_i^t)$
    Set $\boldsymbol{x}_i^{t+1} = \boldsymbol{x}_i^t + \boldsymbol{v}_i^{t+1}$
  end for
  Set $t = t + 1$
  Set $\boldsymbol{sol} = \operatorname{argmin}_{p_i \in \mathcal{P}} f(\boldsymbol{pb}_i^t)$
until $f(\boldsymbol{sol})$ value is good enough or $t = t_{max}$

According to Fig. 7, the algorithm needs more exploratory configurations

information web page [20].

(i.e., fast topology update schedules and slow inertia weight schedules) for long runs. For short runs, configurations with slow topology update schedules and fast inertia weight schedules yield the best results. For runs of 10^4 and 10^5 function evaluations, the best configurations are intermediate ones (i.e., fast or slow schedules for both the topology and inertia weight updates).

The more exploratory behavior that a large population provides needs to be counterbalanced by the chosen configuration. For example, at 10^3 function evaluations, the best configuration tends to have faster inertia weight schedules for larger swarms. With 20 particles, the best configuration is at point $(4, 3)$ while with 40 and 60 particles, the best configurations are at $(4, 2)$ and $(4, 1)$, respectively. These results are consistent with those of the experimental comparison.

Like any other algorithm, Frankenstein's PSO has its own set of parameters that need to be set by the practitioner before trying to solve a problem. The final parameter settings will depend on the class of problems one is trying to solve and on the application scenario requirements. The results presented in this section serve only to understand the behavior of the algorithm when different parameterizations are used.

6 Performance Validation

The performance of Frankenstein's PSO is evaluated by comparing its best configurations with those of the PSO algorithms described in Section 4. To do so, we first identify the best configurations of every PSO variant as a function of the maximum number of function evaluations in a way analogous to Section 4.2. (We select candidate configurations for each PSO algorithm separately to avoid artificially favoring some PSO variants because of having more representatives in the ranking.) For each PSO algorithm we consider all its configurations resulting from our experimental setup and we choose, for each termination criterion, the best performing ones. Table 7 shows these best configurations (from those tested) for each PSO algorithm and termination criterion.

In a second step, we compare the algorithms' configurations shown in Table 7. For this purpose, and to be able to compare their relative effectiveness, we standardize the median solution qualities achieved by each of them. Table 8 shows the standardized median solution quality obtained by each configuration (identified only by the algorithm's name) for each termination criterion. The best values for each individual problem and stopping criterion are highlighted in boldface.

Table 7: Best configurations of different PSO variants for different termination criteria

FES	Algorithm	Configuration			
		Particles (n)	Topology[1]	Topology Schedule	Inertia Weight Schedule
10^3	Constricted	20	F	-	-
	Decreasing-IW	20	F	-	10^2
	Increasing-IW	20	F	-	10^5
	Stochastic-IW	20	F	-	-
	FIPS	20	S	-	-
	HPSOTVAC	20	S	-	-
	AHPSO	20	T	-	-
	Frankenstein's PSO	20	T	$4n$	$3n^2$
10^4	Constricted	20	S	-	-
	Decreasing-IW	20	F	-	10^3
	Increasing-IW	20	S	-	10^6
	Stochastic-IW	20	S	-	-
	FIPS	20	R	-	-
	HPSOTVAC	20	S	-	-
	AHPSO	40	T	-	-
	Frankenstein's PSO	20	T	$4n$	$4n^2$
10^5	Constricted	40	S	-	-
	Decreasing-IW	60	F	-	10^4
	Increasing-IW	60	F	-	10^6
	Stochastic-IW	20	S	-	-
	FIPS	40	R	-	-
	HPSOTVAC	20	R	-	-
	AHPSO	60	T	-	-
	Frankenstein's PSO	20	T	$4n$	$3n^2$
10^6	Constricted	60	S	-	-
	Decreasing-IW	40	R	-	10^5
	Increasing-IW	60	S	-	10^6
	Stochastic-IW	60	S	-	-
	FIPS	40	R	-	-
	HPSOTVAC	40	S	-	-
	AHPSO	60	T	-	-
	Frankenstein's PSO	60	T	$2n$	$4n^2$

[1] F, S, R, T stand for fully connected, square, ring, and time-varying, respectively.

Table 8: Best overall configurations of different PSO variants for different termination criteria. Each group is sorted by the average standard solution quality in ascending order, so the best overall configuration is listed first

FES	Algorithm	Ackley	Griewank	Rastrigin	Salomon	Schwefel	Step	Rosenbrock	Sphere	Average
10^3	Frankenstein's PSO	**-2.024**	**-0.955**	-0.975	**-0.517**	1.378	**-1.315**	-0.302	**-1.108**	-0.727
	Increasing-IW	-0.013	-0.393	-0.950	-0.323	**-1.229**	-0.645	-0.367	-0.371	-0.536
	Decreasing-IW	-0.002	-0.386	**-1.067**	-0.316	-1.199	-0.359	-0.474	-0.425	-0.528
	FIPS	-0.765	-0.430	-0.080	-0.457	1.432	-0.932	0.206	-0.538	-0.195
	Constricted	0.476	-0.156	0.287	-0.276	-0.213	0.406	**-0.491**	-0.057	-0.003
	Stochastic-IW	0.656	0.124	0.652	-0.237	-0.046	0.693	-0.488	0.304	0.207
	AHPSO	0.476	-0.156	0.287	2.464	-0.213	0.406	**-0.491**	-0.057	0.340
	HPSOTVAC	1.198	2.353	1.847	-0.338	0.090	1.745	2.406	2.251	1.444
10^4	Increasing-IW	-0.129	-0.564	-0.593	-0.349	**-0.797**	-0.539	-0.348	-0.359	-0.460
	Constricted	-0.212	-0.616	-0.591	-0.373	-0.459	-0.539	-0.376	-0.359	-0.441
	Decreasing-IW	-0.065	-0.518	**-0.962**	-0.341	-0.754	-0.085	-0.370	-0.358	-0.431
	Frankenstein's PSO	**-1.061**	**-0.761**	0.056	**-0.386**	1.332	**-0.993**	**-0.414**	**-0.361**	-0.324
	Stochastic-IW	-0.131	0.443	-0.512	-0.361	-0.541	-0.085	-0.290	-0.359	-0.230
	FIPS	-1.056	-0.718	1.567	-0.378	1.760	-0.539	-0.364	**-0.361**	-0.011
	AHPSO	0.569	0.656	-0.512	2.474	-0.641	0.596	-0.312	-0.316	0.314
	HPSOTVAC	2.086	2.077	1.546	-0.287	0.101	2.185	2.473	2.475	1.582
10^5	Frankenstein's PSO	**-0.354**	**-0.883**	-1.192	**-0.359**	**-1.548**	-0.487	0.782	**-0.354**	-0.549
	Decreasing-IW	**-0.354**	0.631	-0.709	-0.355	-0.311	**-0.787**	-0.983	**-0.354**	-0.402
	Increasing-IW	**-0.354**	0.631	0.108	-0.355	-0.271	**-0.787**	-0.441	**-0.354**	-0.228
	Constricted	**-0.354**	**-0.883**	0.313	**-0.359**	0.729	-0.487	0.216	**-0.354**	-0.147
	Stochastic-IW	**-0.354**	0.631	1.130	**-0.359**	0.649	**-0.787**	-1.013	**-0.354**	-0.057
	FIPS	**-0.354**	**-0.883**	1.060	-0.355	1.372	0.712	1.008	**-0.354**	0.276
	AHPSO	**-0.354**	1.639	0.721	2.475	0.529	0.712	**-1.019**	**-0.354**	0.544
	HPSOTVAC	2.475	**-0.883**	**-1.431**	-0.334	-1.149	1.911	1.449	2.475	0.564
10^6	Frankenstein's PSO	**-0.354**	**-0.354**	-0.787	**-0.358**	-1.257	**-0.661**	-0.058	**-0.504**	-0.542
	Increasing-IW	**-0.354**	**-0.354**	0.002	-0.354	0.019	**-0.661**	0.039	**-0.504**	-0.271
	Decreasing-IW	**-0.354**	**-0.354**	0.472	-0.354	0.367	**-0.661**	**-0.778**	**-0.504**	-0.271
	FIPS	**-0.354**	**-0.354**	-0.546	-0.354	**-1.349**	0.661	0.685	**-0.504**	-0.264
	Stochastic-IW	**-0.354**	**-0.354**	0.415	**-0.358**	0.705	**-0.661**	-0.529	**-0.504**	-0.205
	Constricted	**-0.354**	**-0.354**	0.815	**-0.358**	1.072	**-0.661**	-0.717	**-0.504**	-0.132
	HPSOTVAC	2.475	**-0.354**	**-1.760**	-0.341	-0.705	0.661	2.129	2.184	0.536
	AHPSO	**-0.354**	2.475	1.388	2.475	1.149	1.984	-0.771	0.840	1.148

For runs of 10^3, 10^5 and 10^6 function evaluations, the best overall configuration is the one of Frankenstein's PSO. For runs of 10^4 function evaluations, the configuration of Frankenstein's PSO is ranked in the fourth place. However, with this same number of function evaluations, the configuration of Frankenstein's PSO is the best configuration in 6 of the 8 benchmark problems. The average rank of Frankenstein's PSO after 10^4 function evaluations can be explained with the results on Schwefel's function: FIPS (of which a component is used in Frankenstein's PSO) is the worst algorithm for this termination criterion (and also for the one of 10^3 function evaluations) on Schwefel's function.

The performance of Frankenstein's PSO suggests that indeed it is possible and profitable to integrate different existing algorithmic components into a single PSO variant. The results show that by composing existing algorithmic components, new high-performance variants can be built. At the same time, it is possible to gain insights into the effects of the interactions of different components on the algorithm's final performance. Of course, just as it is possible to take advantage of the strengths of different components, it is also possible that their weaknesses are passed on. In fact, the performance of Frankenstein's PSO on Schwefel's function is an example of this.

7 Conclusions and Future Work

Many PSO variants are proposed in the current literature. This is a sign of the great attention that PSO has received since its introduction. However, it is also a sign of the generalized lack of knowledge about which algorithmic components provide good performance on particular types of problems and under different operating conditions.

In an attempt to gain insight into the performance advantages that different algorithmic components provide, we compared what we consider to be some of the most influential and promising PSO variants. For practical reasons, many variants were left out of this study. Future algorithmic composition studies should consider other variants in an effort to further understand the interactions among PSO algorithmic components.

The results of the comparison revealed that no variant dominates all the others on all benchmark problems and under all tested circumstances. These results mean that some variants are able to find a solution of a certain quality faster than others, or, given the possibility of using the same number of function evaluations, they are able to find solutions of better quality. Since variants differ on some specific algorithmic components, differences in performance must come from these components and/or the way they interact with others. The question then becomes: Is it possible to combine different algorithmic components that seem to provide good performance into a single PSO variant capable of performing better than the variants from which these components were taken?

The results presented in this paper suggest that the answer to this question is positive. The algorithm that we call *Frankenstein's PSO* is a composite algorithm with three main algorithmic components: (i) a time-varying population topology that decreases its connectivity as the optimization process evolves; (ii) a particles' velocity-update mechanism that exploits every stage of the topology change process, and (iii) a time-decreasing inertia weight that allows the user to tune the algorithm's exploration/exploitation capabilities. Frankenstein's PSO

is capable of performing better than the variants from which its components were taken. These components were chosen after analyzing the results of the empirical comparison.

One algorithmic component that could further improve Frankenstein's PSO performance (or that of other variants), is the use of restarts. In our empirical evaluation, we showed that simple independent restarts can dramatically increase the probability of finding high-quality solutions. Unfortunately, there is no fixed restart policy that would work equally well for all problems or algorithms. A restarting mechanism that uses information collected during the development of the optimization run, that is, an adaptive mechanism, is then a promising research direction that deserves further investigation.

As a methodological approach, algorithm composition can help in identifying positive and negative (in terms of performance) interactions among algorithmic components. Another selection of PSO variants would have probably ended up in a different Frankenstein's PSO algorithm. For this reason, further research is needed to understand which components are better suited for particular classes of problems and operating conditions and whether some components can be integrated into the same composite algorithm or not. Methods to quantify the contribution of each component on the composite algorithms' final performance are also needed to achieve this goal.

Acknowledgment

This work was supported by the ANTS project, an *Action de Recherche Concertée* funded by the Scientific Research Directorate of the French Community of Belgium. Marco A. Montes de Oca acknowledges support from Programme Alβan, the European Union Programme of High Level Scholarships for Latin America, scholarship No. E05D054889MX. Thomas Stützle, Mauro Birattari and Marco Dorigo acknowledge support from the fund for scientific research F.R.S-FNRS of the French Community of Belgium. We thank the anonymous reviewers and the editor for their comments that greatly improved this manuscript.

References

[1] J. Kennedy and R. Eberhart, "Particle swarm optimization," in *Proceedings of IEEE International Conference on Neural Networks*. Piscataway, NJ, USA: IEEE Press, 1995, pp. 1942–1948.

[2] R. Eberhart and J. Kennedy, "A new optimizer using particle swarm theory," in *Proceedings of the 6th International Symposium on Micro Machine and Human Science*. Piscataway, NJ, USA: IEEE Press, 1995, pp. 39–43.

[3] A. P. Engelbrecht, *Fundamentals of Computational Swarm Intelligence*. Chichester, England: John Wiley & Sons, 2005.

[4] R. Poli, J. Kennedy, and T. Blackwell, "Particle swarm optimization. An overview," *Swarm Intelligence*, vol. 1, no. 1, pp. 33–57, 2007.

[5] M. Clerc and J. Kennedy, "The particle swarm–explosion, stability, and convergence in a multidimensional complex space," *IEEE Transactions on Evolutionary Computation*, vol. 6, no. 1, pp. 58–73, 2002.

[6] S.-K. S. Fan and E. Zahara, "A hybrid simplex search and particle swarm optimization for unconstrained optimization," *European Journal of Operational Research*, vol. 181, no. 2, pp. 527–548, 2007.

[7] Y. Shi and R. Eberhart, "Parameter selection in particle swarm optimization," in *LNCS 1447. Evolutionary Programming VII: 7th International Conference*. Berlin, Germany: Springer-Verlag, 1998, pp. 591–600.

[8] R. Eberhart and Y. Shi, "Comparing inertia weights and constriction factors in particle swarm optimization," in *Proceedings of the 2000 IEEE Congress on Evolutionary Computation*. Piscataway, NJ, USA: IEEE Press, 2000, pp. 84–88.

[9] I. C. Trelea, "The particle swarm optimization algorithm: Convergence analysis and parameter selection," *Information Processing Letters*, vol. 85, no. 6, pp. 317–325, 2003.

[10] Y. Shi and R. Eberhart, "A modified particle swarm optimizer," in *Proceedings of the IEEE International Conference on Evolutionary Computation*. Piscataway, NJ, USA: IEEE Press, 1998, pp. 69–73.

[11] ——, "Empirical study of particle swarm optimization," in *Proceedings of the 1999 IEEE Congress on Evolutionary Computation*. Piscataway, NJ, USA: IEEE Press, 1999, pp. 1945–1950.

[12] Y.-L. Zheng, L.-H. Ma, L.-Y. Zhang, and J.-X. Qian, "On the convergence analysis and parameter selection in particle swarm optimization," in *Proceedings of the 2003 IEEE International Conference on Machine Learning and Cybernetics*. Piscataway, NJ, USA: IEEE Press, 2003, pp. 1802–1807.

[13] ——, "Empirical study of particle swarm optimizer with an increasing inertia weight," in *Proceedings of the 2003 IEEE Congress on Evolutionary Computation*. Piscataway, NJ, USA: IEEE Press, 2003, pp. 221–226.

[14] R. Eberhart and Y. Shi, "Tracking and optimizing dynamic systems with particle swarms," in *Proceedings of the 2001 IEEE Congress on Evolutionary Computation*. Piscataway, NJ, USA: IEEE Press, 2001, pp. 94–100.

[15] R. Mendes, J. Kennedy, and J. Neves, "The fully informed particle swarm: Simpler, maybe better," *IEEE Transactions on Evolutionary Computation*, vol. 8, no. 3, pp. 204–210, 2004.

[16] A. Ratnaweera, S. K. Halgamuge, and H. C. Watson, "Self-organizing hierarchical particle swarm optimizer with time-varying acceleration coefficients," *IEEE Transactions on Evolutionary Computation*, vol. 8, no. 3, pp. 240–255, 2004.

[17] S. Janson and M. Middendorf, "A hierarchical particle swarm optimizer and its adaptive variant," *IEEE Transactions on Systems, Man and Cybernetics–Part B*, vol. 35, no. 6, pp. 1272–1282, 2005.

[18] J. J. Liang, P. N. Suganthan, and K. Deb, "Novel composition test functions for numerical global optimization," in *Proceedings of IEEE Swarm Intelligence Symposium.* Piscataway, NJ, USA: IEEE Press, 2005, pp. 68–75.

[19] P. N. Suganthan, N. Hansen, J. J. Liang, K. Deb, Y.-P. Chen, A. Auger, and S. Tiwari, "Problem definitions and evaluation criteria for the CEC 2005 special session on real-parameter optimization," Nanyang Technological University, Singapore and IIT Kanpur, India, Tech. Rep. 2005005, 2005.

[20] M. A. Montes de Oca, T. Stützle, M. Birattari, and M. Dorigo, "Frankenstein's PSO: Complete data," 2007, Supplementary information page at `http://iridia.ulb.ac.be/supp/IridiaSupp2007-002/`.

[21] R. Mendes, "Population topologies and their influence in particle swarm performance," Ph.D. dissertation, Escola de Engenharia, Universidade do Minho, Portugal, 2004.

[22] A. Mohais, R. Mendes, C. Ward, and C. Posthoff, "Neighborhood restructuring in particle swarm optimization," in *LNCS 3809. Proceedings of the 18th Australian Joint Conference on Artificial Intelligence.* Berlin, Germany: Springer, 2005, pp. 776–785.

[23] H. H. Hoos and T. Stützle, *Stochastic Local Search: Foundations and Applications.* San Francisco, CA, USA: Morgan Kaufmann, 2004.

[24] J. Niehaus and W. Banzhaf, "More on computational effort statistics for genetic programming," in *LNCS 2610. Genetic Programming: 6th European Conference, EuroGP 2003.* Berlin, Germany: Springer-Verlag, 2003, pp. 164–172.

[25] M. A. Montes de Oca, T. Stützle, M. Birattari, and M. Dorigo, "A comparison of particle swarm optimization algorithms based on run-length distributions," in *LNCS 4150. Ant Colony Optimization and Swarm Intelligence. 5th International Workshop, ANTS 2006.* Berlin, Germany: Springer-Verlag, 2006, pp. 1–12.

[26] P. N. Suganthan, "Particle swarm optimiser with neighbourhood operator," in *Proceedings of the 1999 IEEE Congress on Evolutionary Computation.* Piscataway, NJ, USA: IEEE Press, 1999, pp. 1958–1962.